Review

A Review of Condensation Frosting—Mechanisms and Promising Solutions

Tian Gu [1], Yugang Zhao [1,2,*], Yusheng Liu [1] and Dongmin Wang [1]

1 Shanghai Key Laboratory of Multiphase Flow and Heat Transfer in Power Engineering, School of Energy and Power Engineering, University of Shanghai for Science and Technology, Shanghai 200093, China
2 Key Laboratory of Icing and Anti/De-Icing, China Aerodynamics Research and Development Center, Mianyang 621000, China
* Correspondence: ygzhao@usst.edu.cn

Abstract: Icing in the form of condensation frosting occurs ubiquitously in our daily life and numerous industrial applications. As the frost layer mostly comprises mixed microscopic dendrites and discrete air pockets, condensation frosting manifests a thick porous media and thus catastrophically compromises the heat transfer efficiency of HVAC systems. Despite being a popular research topic for centuries, a few unprecedented advances in the study of condensation frosting have been only achieved very recently, such as the revealing of new features in the incipient stages of frost formation, which used to be too fast or too small to capture, and new anti-/de-frosting techniques have been developed based on the revealed physics. This work provides a comprehensive, up-to-date review of condensation frosting, with an emphasis placed on progress in the very latest decade. Fundamentals of condensation frosting, including condensation nucleation, coalescence and growth of the condensed drops, icing nucleation, formation of frost halos, freezing propagation via ice bridging, and lastly densification and fully developed frost layers, are introduced chronologically as what occurs. A summary of recent engineering efforts to alleviate the negative impacts of condensation frosting, referred to as anti-/de-frosting techniques, is also presented. The results of these studies can greatly enlighten the existing understanding of condensation frosting and, meanwhile, benefit the development of new anti-/de- frosting methods for numerous application backgrounds.

Keywords: condensation frosting; interfacial phenomena; frost characteristics; anti-/de-frosting techniques

1. Introduction

Dated back to 1888, more than 130 years ago, Mr. A.N.S. saw the beautiful appearance of snowflakes glowing in the dark night when exposed to sunlight, raising a few questions about how these crystals are formed and why they look so fascinating [1]. It has been a remarkably long history since people started to dig into one of the most ubiquitous phenomena encountered in nature and human activities, i.e., how water vapor gets frozen and the consecutive processes such as the formation of frost, atmosphere icing (snow/hail/rime/frozen rain), accretion of frost in HVAC (heating, ventilating, and air conditioning) systems, and snow/ice making in sports and entertainment business [2,3]. Condensation frosting is one of the most pervasive types of ice that we encounter in many application backgrounds. The structural integrity and mechanical reliability of infrastructures and facilities, such as power transmission systems [4,5], aircraft, and wind turbines [6,7], can be compromised to a considerably large extent due to frost accretion whenever exposed to humid and supercooled environments. For heat transfer equipment such as refrigerators and heat pumps, both their heat transfer efficacy and capacity will be tremendously reduced once the interfaces are covered by thick porous frost layers [8–11]. Billions of economic losses or even the cost of human lives due to frost/ice accretion have occurred multiple times, such as the cold weather strike across southern China in 2018 and the Texas power crisis in 2021.

Although we have come a long way since we noticed this intriguing phase-change phenomenon, tried to explore the associated physics, and proposed promising strategies to alleviate its negative impacts, our understanding of the physics associated with condensation frosting is still quite limited, and we are far from solving the frosting problem. A great number of unprecedented advances in the study of condensation frosting have been only achieved very recently. For instance, we used to believe icing nucleation in condensation frosting takes place in isolation by heterogeneous nucleation at the liquid–substrate interface among a collection of condensed drops [12]. Dooley [13] and later Guadarrama-Cetina et al. [14] found that small dendrites originated from a frozen drop contact physically with its neighboring liquid drops to trigger them to freeze, resulting in a chain-like reaction, referred to as freezing propagation. The revealing of freezing propagation dynamics, along with other associated phenomena such as coalescences-induced spontaneous drop jumping, two distinguished freezing stages of a sessile supercooled drop, and frost halos, significantly reshaped our understanding of condensation frosting. Additionally, owing to the recent development of surface engineering and microfabrication technologies [15–18], tailoring surface chemistry and topological features to obtain superwettability to suppress frost formation, termed anti-frosting approaches, has received growing attention in this very decade. Compared to conventional de-frosting approaches, which solve the frosting problem by promoting frost removal/drainage using thermal/mechanical/chemical ways, anti-frosting approaches have already shown many clear advantages such as no requirement of external energy/chemical input [19], economically effective, and eco-friendly, to name but a few.

Compared to other phase-change phenomena such as condensation, evaporation, and boiling, icing, or more specifically condensation frosting, is undoubtedly the new hot spot in thermal physics. Much greater progress has been made on condensation frosting in the past decade, from both the fundamental studies of its physics and the application of technologies aiming to address the frost challenge. Our work herein aims to provide a comprehensive, up-to-date review of the literature on the recent progress of condensation frosting. This review is organized as follows: Section 2 gives modified physical descriptions of condensation frosting dynamics. Section 3 provides newly developed approaches to solve the frost accretion problem with a special focus placed on anti-frosting methods. Lastly, we conclude this review and provide our perspectives on this topic.

2. Mechanism of Condensation Frosting: 5 Consecutive Stages

Condensation frosting is a complex heat and mass transfer process composed of two steps of phase change: condensation when ambient vapor becomes oversaturated and nucleates on the liquid–substrate interface, and icing when condensed drops freeze and subsequently frost dendrites grow atop frozen drops. Although the occurrence of desublimation, i.e., vapor directly turns to ice on sufficiently hydrophilic surfaces and at cold enough temperature (contact angle smaller than $50°$, substrate temperature lower than $-35\ °C$) [20], is also widespread, in this work we solely focus on the more general cases of condensation frosting. As shown in Figure 1, we characterize the whole physical process chronologically into five sequential stages: (I) nucleation, growth, and coalescence of condensed drops; (II) icing in one of the condensed drops; (III) evaporation-induced condensation/frost halos; (IV) freezing propagation via ice bridging; and (V) growth of ice dendrites and frost densification.
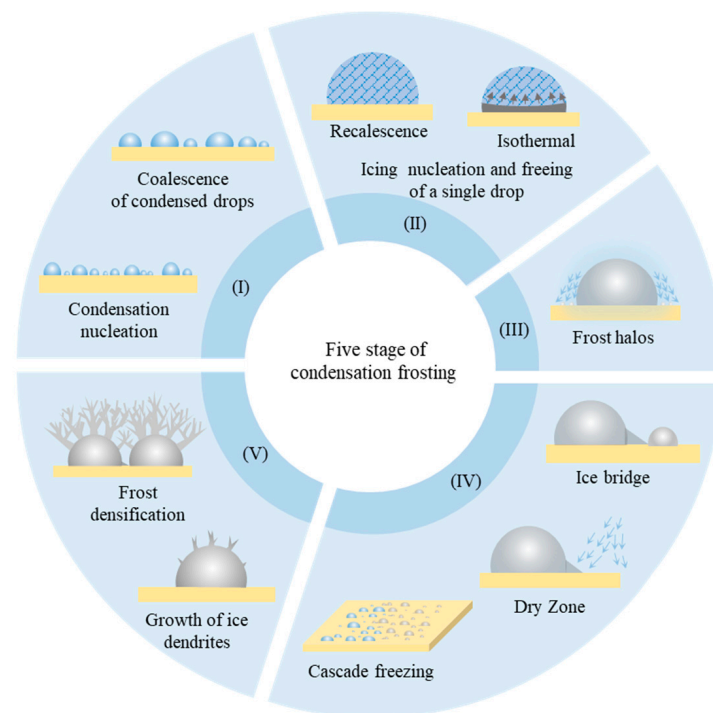
Figure 1. Five physical stages of condensation frosting.

2.1. Condensation Nucleation and Interdrop Coalescences

Condensation refers to the formation of nanoscale liquid condensate once its vapor is oversaturated, or in other words, the solid surface is supercooled for the heterogeneous mode. For water vapor specifically, a certain degree of supercooling beneath the dew point is necessary to overcome the heterogeneous energy barrier ΔG_{Hetero} required to create a stable nucleating embryo (with a minimal radius $r \geq r_{cri}$, r_{cri} being the critical radius for condensation nucleation).

As the incipient stage of the whole physical process, the location and density of nucleation sites dominate the distribution of condensate, which in turn plays a decisive role in successive frosting stages. Both surface chemistry and topological features can be tailored to modulate condensation dynamics. Boreyko et al. used engineered surfaces carrying solely chemical patterns to spatially control the nucleation sites [21]. Arrays of hydrophilic dots were patterned again on a hydrophobic background, engendering a typical wettability contrast. As shown in Figure 2a, the energy barrier for condensation nucleation in hydrophilic regions is significantly smaller than that of hydrophobic regions, providing preferential nucleation sites where stable condensed drops emerge and start to grow bigger in size. Zhao et al. fabricated silicon-based topological patterns to control the size and distribution of condensed drops [22,23]. As shown in Figure 2b, micropillar patterned surfaces with varying diameters and pitches were fabricated using standard photolithography. The prepared surfaces are macroscopically superhydrophobic if placing a millimeter-sized water drop atop. As the surface is chemically homogeneous, condensation nucleation occurs uniformly on the substrate bases, as well as the pillar tops and sidewalls. However, condensed drops atop pillars are subjected to much larger feeding flux, and thus can grow faster. Accordingly, we can observe that pillar tops collect most of the condensate in the late stage of condensation. Recently, engineered surfaces with both chemical and topological patterns were also exploited. Hou et al. designed and fabricated a surface that carries a biphilic topography with patterned high-contrast wettability [24]. As shown in Figure 2c, the prepared surface is composed of arrays of hydrophilic micropillars and superhydrophobic nanograss. The condensation dynamics on this biphilic surface were captured via environmental scanning electron microscopy (ESEM). Condensate drops preferentially nucleate atop hydrophilic pillar tops, and superhydrophobic nanograss assists the drops remaining suspended.
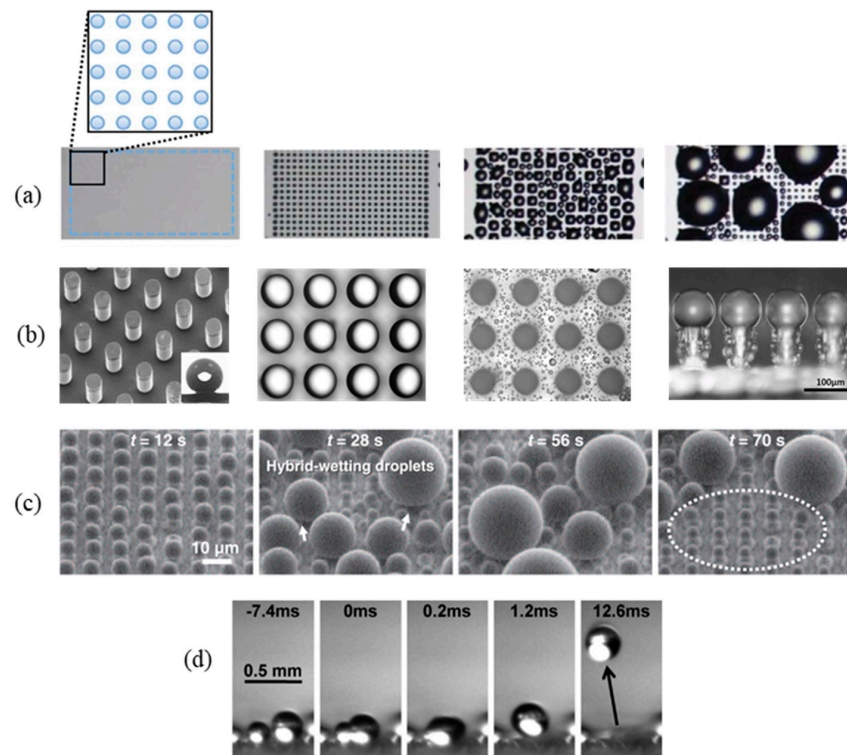
Figure 2. Microscopic condensation dynamics on various types of surfaces. (**a**) chemical patterned surface, Reprint from [21], Copyright 2016 with permission from Springer Nature. (**b**) topologically patterned surface, Reprint from [23], Copyright 2017 with permission from Elsevier. (**c**) biphilic surface with hydrophobic nanograss and hydrophilic micropillars. Reprinted with permission from [24], Copyright 2018 with permission from American Physical Society. and (**d**) spontaneous drop jumping upon coalescence, Reprinted with permission from [25], Copyright 2009 by the American Physical Society.

As condensation proceeds and more vapor is fed continuously, condensate drops grow larger in size and merge with neighboring drops, which is usually termed interdrop coalescence. Accordingly, we believe the transition from dropwise condensation to filmwise condensation is inevitable without applying external forces. Boreyko and Chen found that continuous dropwise condensation is possible on properly designed superhydrophobic surfaces [25]. Condensate drops can jump spontaneously upon the coalescence with neighboring drops due to the release of excess surface energy. As shown in Figure 2d, a surprising out-of-plane jumping motion with a speed up to 1 m/s can result from an in-plane coalescence of two micrometer-sized drops. Later, they further implant this mechanism into phase-thermal thermal diodes to promote heat transfer efficiency with a strong directional preference [26]. Nenad et al. discovered that jumping drops carry a net positive charge, yielding a self-repelling behavior in the mid-fight [27]. They used externally applied electric fields to modulate the kinetics of jumping drops and, more specifically, to increase the jumping frequency from the substrate to promote condensation heat transfer.

2.2. Icing Nucleation and Freezing of a Single Drop

As deduced from Fletcher's classical nucleation theory [28], icing nucleation occurs inside condensed drops at energetically preferential sites, analogous to that of condensation nucleation. For icing nucleation in supercooled sessile drops, there has been a long-lasting debate about whether the triple line is the spatial preferential nucleation site. Gurganus et al. developed a direct experimental approach to study the spatial distribution of nucleation sites for a sessile supercooled drop [29,30]. Two high-speed cameras from both the top view and side view allow pinpointing precisely the location and growth dynamics of the ice embryo. The hexagonal ice crystal initiates from an arbitrary location at the liquid–solid interface, showing that icing nucleation has no preference for the triple line.

Different from the scenario of the freezing of an impinging drop, condensed drops are sessile and supercooled before icing nucleation initiates. Despite that nucleation sites also locate at the liquid–solid interface, the whole freezing dynamics can be very different. Jung et al. found that the freezing process of a sessile supercooled drop proceeds in two consecutive stages, termed the recalescence stage and the isothermal stage, respectively [31]. In the first recalescence stage, a rapid partial freezing occurs, and the whole drop space gradually becomes cloudy as freezing proceeds. Most of the released latent heat is absorbed by the remaining water to raise its temperature, while a small portion is dissipated to the surroundings. In the second isothermal stage, the remaining water gradually transits into a solid, filling the crystalline gaps formed during the recalescence stage. The released latent heat in this stage is mostly transferred to the substrate base. In general cases, the isothermal stage proceeds near 3 orders of magnitude slower than the recalescence stage.

An intriguing fact about water is it expands upon freezing, and thus the shape of a drop evolves as freezing proceeds. Marín et al. carried out a set of experiments to study the shape of frozen drops, and proposed a quantitative description [32]. For both 3D drops and 2D drops (as confined in a Hele–Shaw geometry), the top portion of a frozen drop is a conical tip, which is independent of contact angle and substrate supercooling temperature.

2.3. Freezing Halo

The formation of frost halos initiates at the onset of icing nucleation, and thus chronologically is partially overlapping with the drop icing stage. Before the recent work by Jung et al. [33], people used to formulate frost halos as the result of the spontaneous ejection of micrometer-sized drops when a large drop starts to freeze. An appreciable amount of vapor is released from the air–liquid interface when the main drop freezes and heats up the remaining liquid. This vapor becomes locally supersaturated and deposits surrounding the main drop, engendering a halo consisting of micrometer-sized condensate drops. These condensate drops inside the halo are either frozen into ice drops forming so-called frost halos, or evaporated off if too remote from the main drop. Vapor from the evaporated remote condensate drops is transferred via diffusion and redeposited on the neighboring frost halo. Furthermore, they compared the halo formation on surfaces with varying thermal conductivity. On low thermal conductivity materials, the freezing time of the main drop is longer, and thus more evaporated vapor is released. Condensed drops can grow, coalesce, and freeze, yielding a large freezing halo. On high thermal conductivity materials, the main drop freezes drastically faster, cutting off the source of feeding vapor flux. More condensed microdrops are evaporated off before freezing, yielding a small freezing halo.

Note that when one single drop among condensed drops gets frozen, ice covers not only the frozen drop itself, but also a radial area to an appreciable extent, explaining why frost coverage is significantly larger than condensate coverage for the same thermal physical circumstances. Such frost halos were also reported recently by Zhao et al. when they deposited a warm drop onto supercooled surfaces [34]. Even for the case of a surface temperature higher than the freezing point, a similar halo-like configuration was observed, whereas frost halos transit into condensate halos instead [35].

2.4. Freezing Propagation via Ice Bridging, Dry Zones

As late as 2010, people started to notice that icing in condensation frosting follows a pattern instead of a collection of individual incidences [13,36]. Interdrop dynamics, referred to as freezing wave or ice bridging, are exploited to describe the process of how an ice dendrite initiated from a frozen condensate extends to contact with neighboring liquid drops and freezes them. Accordingly, icing nucleation only occurs in energetically preferential sites such as topological cavities and chemical defects, and then limited frozen condensates set off a chain reaction spreading over whole supercooled surfaces.

Ice bridging is a multistep phase-change phenomenon coupled with spatial and temporal variations of heat and mass transfer, and thus a quantitative physical description that matches experimental observations is impractical. Boreyko and Collier employed a simplified

two-dimensional physical model to describe how a typical ice bridge is constructed, as shown schematically and experimentally in Figure 3a,b, respectively [37]. Once a condensate drop is frozen, a vapor concentration gradient is built between its ice interface and neighboring liquid interface. The neighboring liquid drop evaporates, and the evaporated vapor is deposited onto the frozen drop to construct the ice bridge. As the evaporation and the deposition proceeds, the ice dendrite expands towards the neighboring drop, which meanwhile shrinks in size due to the evaporative loss of mass. A scaling analysis that correlates the dendrite growth rate and the evaporative mass loss can be applied to evaluate the time scale to construct the ice bridge. Note that a frozen drop has multiple neighboring liquid drops and vice versa, and a sequence presents when frost spreads across a group of condensate drops. Guadarrama-Cetina et al. experimentally investigated the routine of frost spreading when 2D ice bridges percolate through a network of condensate drops [14]. A growing dendrite points to the neighboring liquid drop and a successful ice bridge is constructed if the liquid drop is sufficiently close and large enough. A failed percolation, or a partially constructed ice bridge, occurs when the liquid drop is evaporated off before any dendrite reaches. Accordingly, a considerable number of liquid drops that are too small in size and too remote vanish during frost spreading, leaving depleted dry zones around the frozen drops and ice bridges. Hauer et al. studied the pattern formation in frost spreading using laser-induced fluorescence microscopy [38]. Varying modes of frost spreading on microstructured surfaces were revealed by setting the degree of supercooling and the time of condensation.
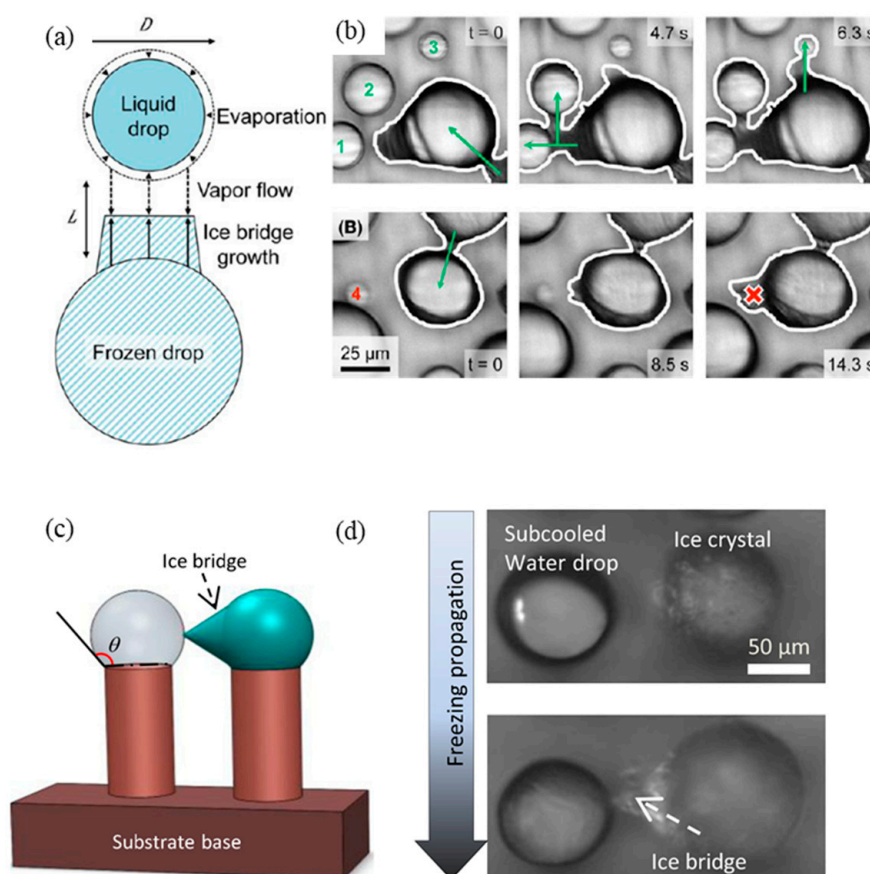
Figure 3. Ice bridging dynamics on smooth and topologically patterned surfaces. (**a**) Schematics of a flat ice bridge connecting two neighboring drops, Reprinted with permission from [37], Copyright 2013 American Chemical Society. (**b**) A network of 2D ice bridges connecting multiple supercooled drops observed in experiments, Reprinted with permission from [37], Copyright 2013 American Chemical Society. (**c**) Schematics of a conical ice bridge connection two suspended drops, Reprint from [22], Copyright 2016 with permission from AIP Publishing. (**d**) growth dynamics of a 3D ice bridge captured in experiments, Reprint from [22], Copyright 2016 with permission from AIP Publishing.

The scenario becomes drastically different when condensate drops are suspended. Zhao et al. developed an analytical model to describe quantitatively the time required to construct a 3D ice bridge [22,39]. A series of silicon-based micropillar patterned surfaces were employed to control precisely the size and distribution of condensate drops. Icing nucleation occurs at substrate edges which carry topological defects, allowing us to further control the direction of ice bridging. As shown in Figure 3c,d, the geometry of a typical 3D ice bridge is considered to be of a circular cone. They also assumed that vapor transfer is governed by one-dimensional diffusion. The time required to construct one single ice bridge can be computed by balancing the mass transfer rate and the total bridge mass, based on which a spatial average frost spreading velocity can be obtained.

2.5. Dendrite Growth Atop Frozen Drop and Densification

As a conical tip presents atop the frozen drop due to the volume expansion upon freezing, this phenomenon engenders an interesting consequence in the succeeding growth of ice dendrites when dealing with condensation frosting. The singular tip is exposed to a significantly large feeding flux driven by the vapor concentration gradient, making it a preferential site for vapor deposition (physically can be termed desublimation [40]). Accordingly, ice dendrites grow like a tree, as reported by Enriquez et al. [41]. Yu et al. measured quantitatively the growth dynamics of ice dendrites atop frozen drops at varying supercooling temperatures, as shown in Figure 4a [42]. In general cases of ordinary-low temperatures, needle dendrites grow into columnar shapes, and their tips melt when exposed to thermal fluctuations. Their upper interfaces gradually change into lumps, and overall dendrites grow into larger sizes. At relatively lower cryogenic temperatures, the growth of ice dendrites is much slower. Vapor is frozen into ice clusters and deposited atop the drop instead. As frosting proceeds, thicker ice clusters cover the drop and inhibit the growth of dendrites. Huang et al. further evaluated the effect of surface orientations with respect to gravity on the growth rate of ice dendrites as vapor transfer occurs via natural convection, as shown in Figure 4b [43]. They found both the average vapor deposition rate and its spatial variation change profoundly by altering surface orientation. For a horizontally placed surface, detectable dendrites grow all over the frozen drop, with an appreciable larger growth rate at the singular tip, named the "global peak". Later, vapor deposition near the global peak is suppressed to some extent, yielding two secondary "local peaks". For a vertically placed surface, the frozen drop is unsymmetrical due to the effect of gravity. Ice embryos emerge only at the upper portion of the frozen drop, and eventually, only the upper portion is covered with a collection of ice dendrites, leaving a smooth ice-air interface for the bottom portion of the frozen drop. The results show that natural convection can either assist or hinder the vapor diffusion process, and affect the deposition outcomes.

Once the entire surface is covered by a network of frozen drops and ice bridges, dendrite growth atop the frozen phase leads to crossing, reverse melting, and collapses, and thus frost density evolves over time [44–48]. Different from other incipient condensation frosting stages, frost densification has been studied extensively for decades. Hermes et al. developed a physical model to describe the variation of the frost density over time based on the mass and energy balances within the frost layer [49]. In such cases, the frost layer is assumed as a porous medium exposed to supersaturated moist air. Song et al. experimentally measured the frost density at varying surface supercooling temperatures [50]. They found that the reverse melting can profoundly increase the frost density, and thus the obtained frost density increases with the increase of the surface temperature. Wang et al. studied experimentally the effect of surrounding humidity on frost density [51]. For larger humidity, more water vapor penetrates the frost interface and diffuses into the inside layer in the desublimation form, yielding a larger frost density. Shin et al. studied the effect of surface wettability on frost density [52]. Their experimental results show hydrophobic surfaces allow the presence of large irregular ice crystals in the earlier stage of frost deposition, and thus result in a low frost density. Thermal physical properties such as thermal

conductivity, heat transfer coefficient, and thermal capacity, depend strongly on the frost density. Therefore, in view of anti-frosting technical attempts, proper design to increase frost density is preferred for HVAC devices.
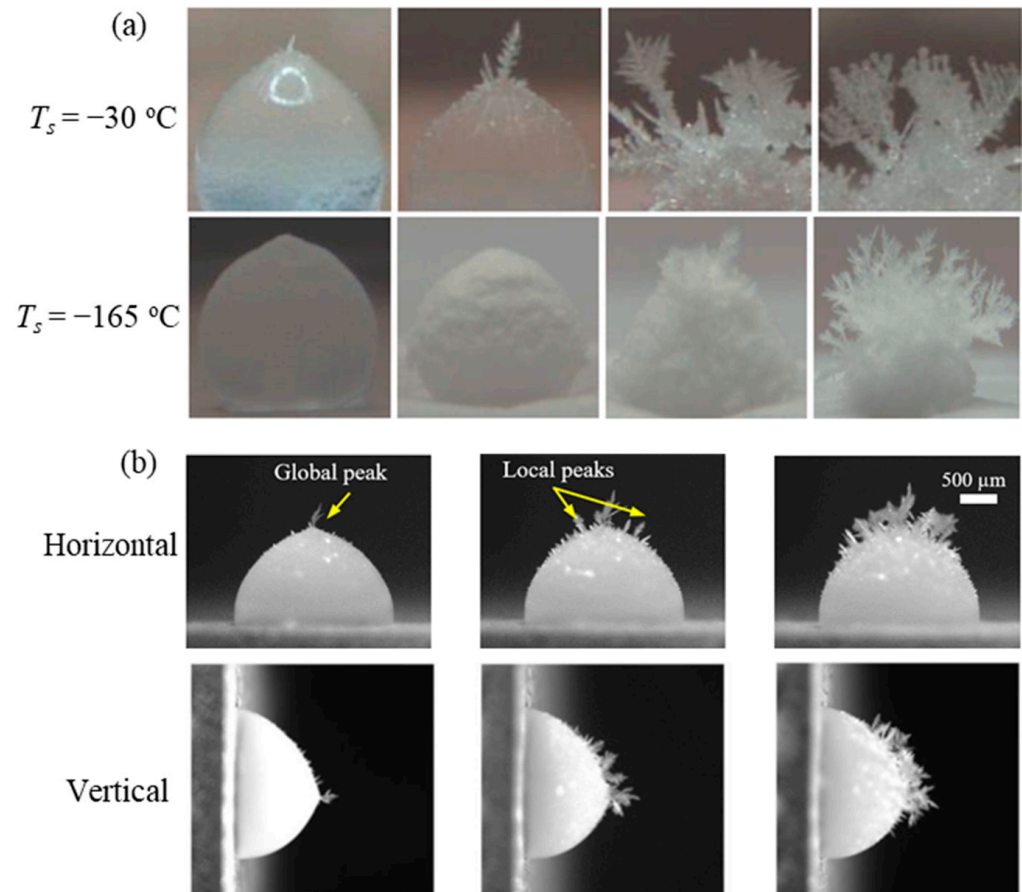
Figure 4. Growth dynamics of ice dendrites atop a frozen drop. (**a**) at an ordinary-low temperature of −30 °C or a cryogenic temperature of −165 °C, Reprint from [42], Copyright 2022 with permission from Elsevier. (**b**) placed horizontally or vertically, Reprint from [43], Copyright 2022 with permission from MDPI.

3. Attempts to Solve Frosting Problems

3.1. Conventional Anti-/De-Frosting Methods

Frost accretion is detrimental and thus undesired in most applications. Ever since studying its underlying mechanism, most of the research attention is placed on how to prevent its occurrence, or alleviate its negative impact. Over the past decades, numerous methods have been developed to prevent frost accretion or to eliminate accreted frost layers. Based on the philosophy selected, these methods can be categorized into two groups: anti-frosting methods, which aim to prevent frost accretion; and de-frosting methods, which aim to promote rapid removal of accreted frost layers.

Conventional de-frosting methods have been very popular for a relatively long history. Selective heating is one of the most common de-frosting methods. The source of heat can vary from the Joule effect induced by electrical conductors, warm air flow, to microwaves, to keep the temperature of protected surfaces slightly above 0 °C [6]. Selective heating is very energy intensive, and thus it is not economically efficient. Chemical spray is another active anti-icing method. The icing nucleation temperature of mixtures can be drastically reduced when adding some chemicals into water, i.e., the freezing point depression. Such chemicals include calcium chloride, methanol, glycerol and glycols, etc. As the magnitude of the freezing point depression decreases almost linearly with the chemical concentration

at low concentrations [19], and the mixture is continuously diluted during the operation as the result of incoming frost melt and chemical drainage, more chemicals need to be added periodically to maintain proper de-frosting performance. Electromagnetically induced vibration is a newly developed active de-icing method, where vibration pulses flex the surface and crack the covered frost layers [53,54]. It occurs when a spiral coil is placed near a metal surface, and a magnetic field is generated when current passes the coil. This magnetic field yields a rapid displacement of the surface, and detaches the accreted frost. One important advantage of this method is that it does not require modifying the surface of equipment.

3.2. Anti-Frosting Methods via Delaying Icing Nucleation

One effective way to prevent frost accretions is to delay the occurrence of icing nucleation. The longer the supercooled surface can stay in the condensation stage, the less frost is accreted, and thus more heat transfer capacity is preserved.

Hao et al. fabricated a nanoribbon-structured superhydrophobic surface, and tested its anti-frosting performance [55]. As shown in Figure 5a, their results show that jumping condensate drops spontaneously leave the surface and take away dust particles, which are either intentionally introduced or naturally deposited onto the surface. Otherwise, these chemical and topological defects can trigger heterogeneous icing nucleation. Particularly, the surface can stay more than 1 h of frost-free when facing downwards and gravity assists in jumping drops off the surface. Accordingly, one main anti-frosting mechanism of superhydrophobic surfaces is that they can keep the whole surface clean from dust particles. Hou et al. used a surface that carries a biphilic topography with patterned high-contrast wettability to promote self-propelled drop jumping [24]. As the average departing radius is small enough (3 times smaller than the drop freezing length scale), supercooled microdrops launch from the surface before icing nucleation occurs. Therefore, the biphilic surface can remain in a sustainable condensation mode without triggering frosting. Wen et al. also proposed to use a specific type of superhydrophobic surface to delay icing nucleation and meanwhile obtain a profoundly improved heat transfer performance [56]. As shown in Figure 5b, the superhydrophobic surface has a three-dimensional nanowire network, which can effectively accelerate the condensation nucleation-to-departure cycle, and thus prevent microdrops from freezing. Unlike most literature using topologically structured surfaces to prevent frosting by suppressing condensation, this new concept can maintain the surface free of frost for more than 5 h and obtain a tenfold enhancement of heat flux. Jung et al. compared the delay of icing nucleation on smooth hydrophilic surfaces and rough superhydrophobic surfaces [58]. They found that wettable surfaces with nano-meter scale roughness can inhibit icing nucleation for a much longer duration than that of typical superhydrophobic surfaces, as heterogeneous nucleation is suppressed on smooth hydrophilic surfaces. Hence, surface engineering aiming to delay icing nucleation needs to consider both wettability and roughness. Ezzat and Huang's work show that even superhydrophilic polymer brushes can resist the icing nucleation of condensed microdrops [59].

Besides surfaces of superwetabilities, other types of surface designs were also developed to achieve anti-frosting via delaying icing nucleation. Recently, Niroomand et al. reported for the first time the icing delay in condensation frosting using a semipermeable membrane [57]. As shown in Figure 5c, as vapor can transfer through the membrane, the onset of freezing is postponed from only 5 min on the impermeable surfaces to more than 2 h on the membrane with the highest vapor transfer rate adopted. Additionally, the shape and layer structure of the frost layer are remarkably altered using the semipermeable membrane. Bio-products such as anti-freeze proteins [60], polypeptides [61], and metal-catechol complexes [62] can also effectively mediate icing nucleation.
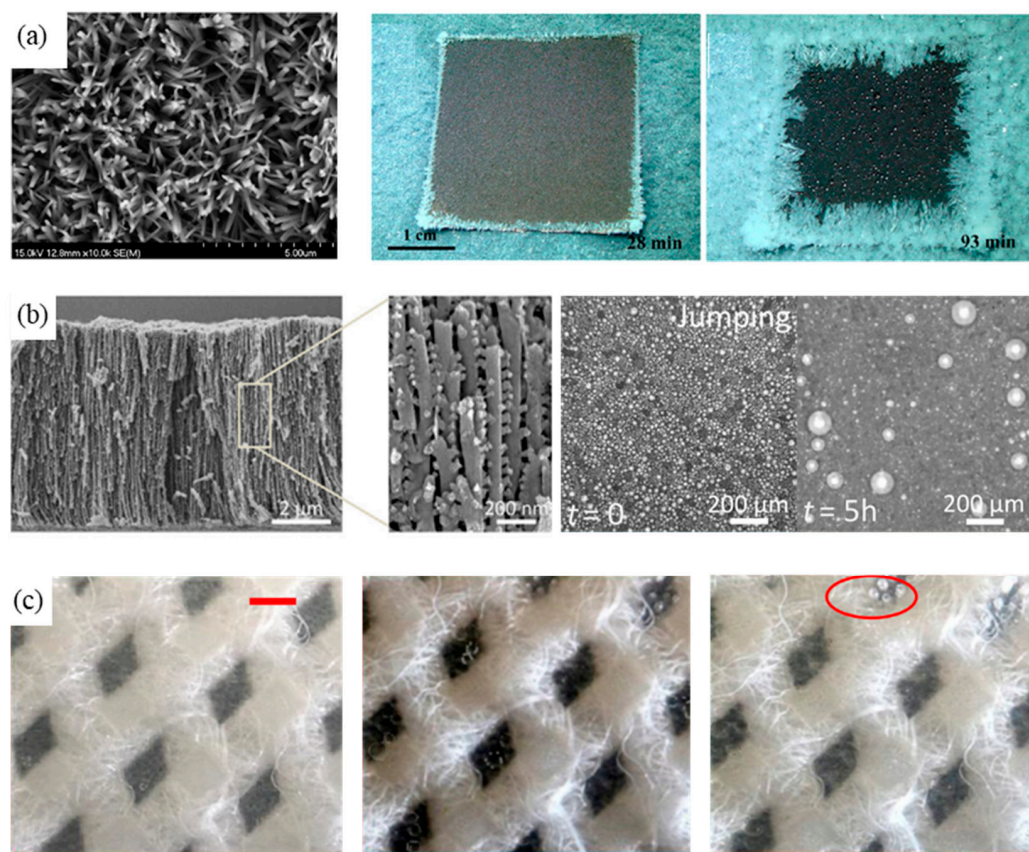
Figure 5. Frosting dynamics for different types of surfaces. (**a**) Superhydrophobic surface carrying nanoribbons, Reprinted with permission from [55], Copyright 2014 American Chemical Society. (**b**) Superhydrophobic surface with a three-dimensional nanowire network, Reprint from [56], Copyright 2022 with permission from Elsevier. (**c**) Semipermeable membrane, Reprint from [57], Copyright 2022 with permission from Elsevier.

3.3. Anti-Frosting Methods via Retarding Freezing Propagation

Another effective way to prevent frost accretions is to retard freezing propagation, i.e., to suppress or even stop the building of ice bridges among condensate microdrops. For a relatively long term since reported, the study on freezing propagation is limited to qualitative descriptions, where the propagation velocity is evaluated from the evolving frost coverage [63–65]. Boreyko et al. studied quantitatively the freezing propagation of a list of chemically patterned surfaces [21]. Instead of waiting for the occurrence of spontaneously heterogeneous icing nucleation at any condensate microdrops, they intentionally triggered icing nucleation by touching the wafer edge using a small piece of ice at the desired time during experiments. As shown in Figure 6a, the freezing phase front propagates almost perpendicularly to the edge, allowing us to measure quantitatively the spatially averaged propagation velocity. They also noticed that the earlier icing nucleation is triggered, the longer time is required for the freezing front to propagate across the surface. Zhao et al. adopt a simple way to evaluate the freeing propagation velocity by selecting the observation window near the edge [39]. As shown in Figure 6b, they compared the measured freezing propagation velocity on microscale wettability and morphology-patterned surfaces. The results show that morphology-patterned surfaces can drastically retard freezing propagation by one order of magnitude via modulating the distribution of condensate microdrops, while the wettability patterned surfaces are less effective.
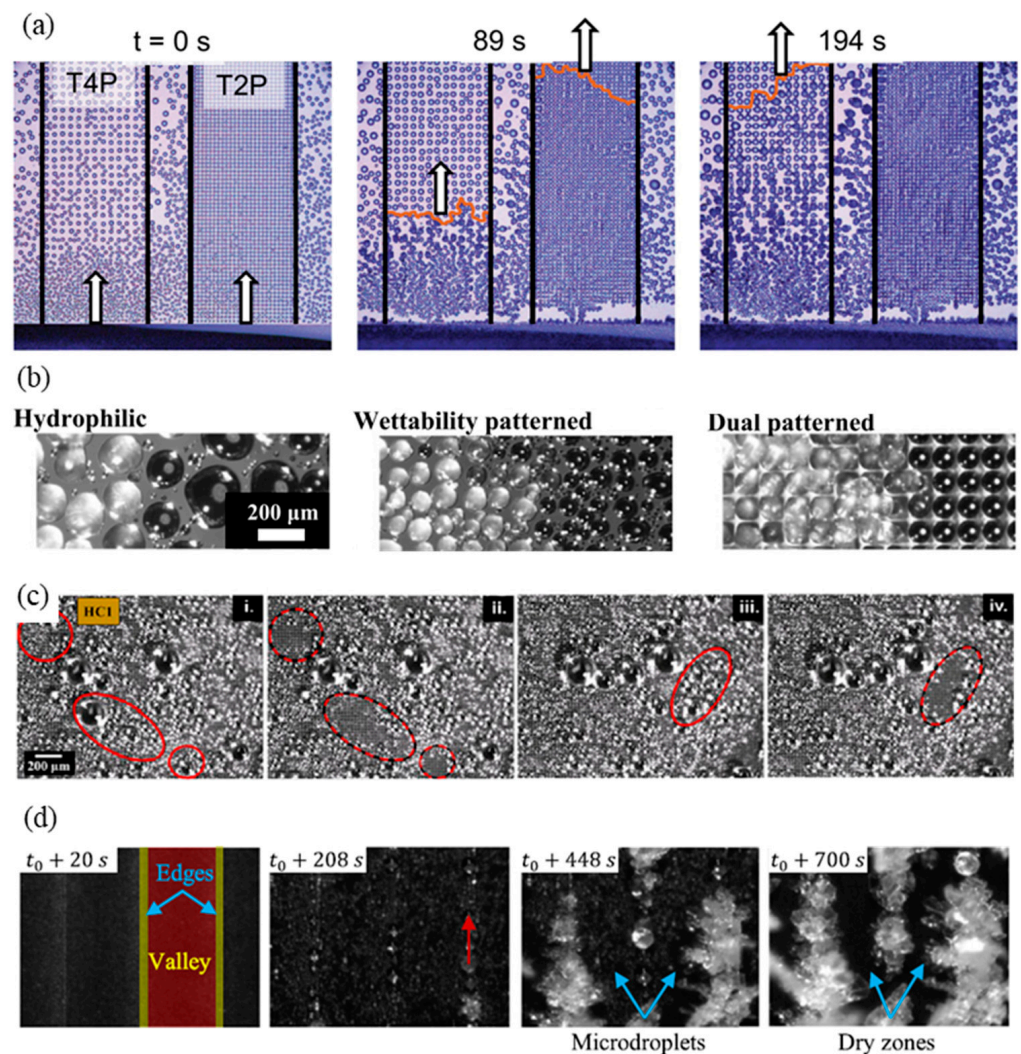
Figure 6. Freezing propagation dynamics on (**a**) the chemically patterned surface, Reprint from [21], Copyright 2016 with permission from Springer Nature. (**b**)wettability/morphology patterned surface, Reprint from [39], Copyright 2017 with permission from Elsevier. (**c**) vertically aligned carbon nanotube based superhydrophobic surface, Reprinted with permission from [66], Copyright 2020 American Chemical Society. and (**d**) copper-based hierarchically structured surface, Reprint from [67], Copyright 2021 with permission from Elsevier.

Besides directly changing the nature of condensation nucleation and vapor deposition, promoting self-propelled drop jumping on superhydrophobic surfaces can also tailor the distribution of condensate drop, and thus affect the building of ice bridges. Mohammadian et al. studied the drop-jumping phenomenon on a vertically aligned carbon nanotube-based superhydrophobic surface and evaluated its effect on the freezing propagation [66]. As shown in Figure 6c, drop jumping together with induced drop sweeping collects all neighboring microdrops, engendering spots of dry zones. These dry spots prevent inter-drop ice bridging from crossing the surface, and thus slow down the overall freezing propagation velocity to 1/3 of that on a smooth untreated surface. Recently, Chu et al. even developed a quantitative correlation between the jumping capacity of microdrops and the freezing propagation velocity [68]. By analyzing three representative parameters, i.e., the drop diameter, the interdrop distance, and the degree of closeness, they obtained the mathematical description of the freezing propagation velocity based on ice bridging theory.

Engineering surfaces with more complex structures have been designed to achieve better anti-frosting performance via further retarding freezing propagation. Yao et al., inspired by the discrete distributed frost pattern on nature leaves, proposed to use the

surface patterned with serrated structures on the scale of millimeters [69]. In the initial stage of condensation frosting, vapor deposition in the form of condensate is enhanced on peaks and suppressed in valleys. During the freezing propagation stage, smaller drops in valleys are evaporated off, producing a millimeter-sized frost-free gap. The freezing phase front cannot cross the gap, and thus frost spreading is constrained locally even on superhydrophilic surfaces. Zhao et al. employed a copper-based hierarchically structured surface to regulate freezing propagation [67]. As shown in Figure 6d, size mismatching among condensate drops is induced by microgroove peaks and nanoblades. Successful ice bridging only occurs along microgrooves, while failing along the perpendicular direction. As the frosting proceeds, only groove peaks are covered with frozen drops and ice dendrites atop in the background of continuous dry valleys.

3.4. Anti-Frosting Methods via Reducing Frost Coverage

Reducing frost (or ice) coverage becomes more applicable when the complete prevention of icing is technologically impossible or economically ineffective. Jin et al. used patterned polyelectrolyte brushes to inhibit condensation frosting as polyelectrolytes can regulate icing nucleation and propagation via changing interfacial counterions [70]. As shown in Figure 7a, icing nucleation only occurs at the top of the polyelectrolytes coated domain, and freezing propagates the rest of the clean surface. Almost all neighboring condensate drops are evaporated off due to the released latent heat and vapor sinks of the frozen drops. An extremely low frost coverage of 4% can be achieved via proper patterning.
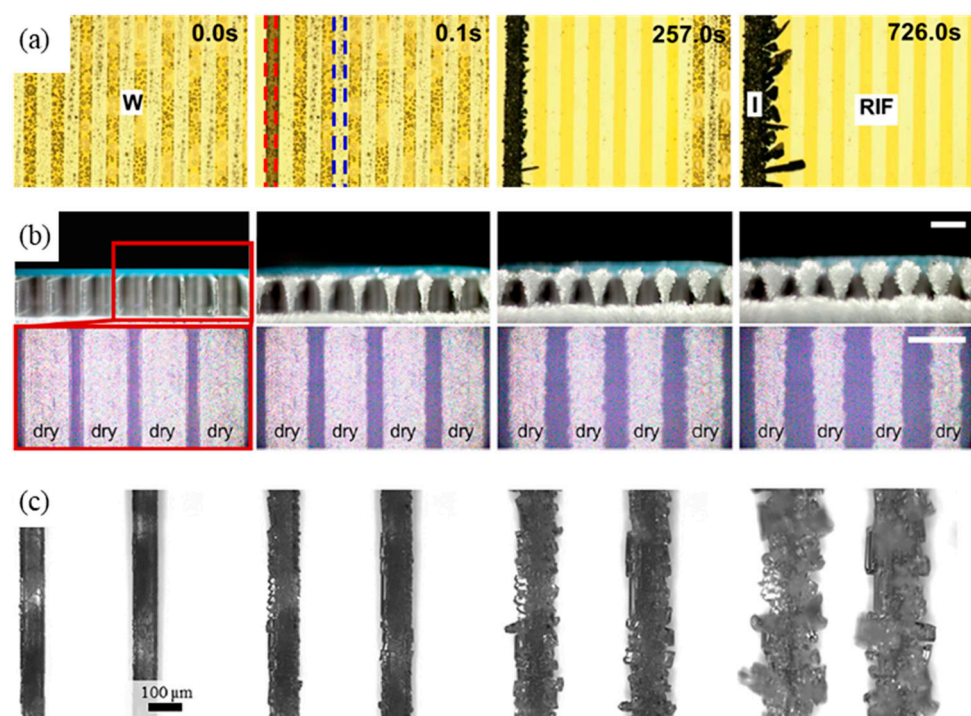
Figure 7. Condensation frosting on (**a**) a polyelectrolyte brush surface, Reprinted with permission from [70], Copyright 2020 American Chemical Society. (**b**) an ice-patterned aluminum surface, Reprinted with permission from [71], Copyright 2018 American Chemical Society. and (**c**) an ice walls patterned surface, Reprint from [72], Copyright 2023 with permission from Elsevier.

Like polyelectrolytes, salts, and glycols, ice is also of a hygroscopic nature, meaning it absorbs moisture from the supersaturated ambient. Ahmadi et al. fabricated an aluminum-based surface with arrays of parallel microgrooves to carry microscopic ice strips [71]. As shown in Figure 7b from both side and top views, the fin tops are treated as sacrificial ice regions that absorb all nearby moisture, leaving the substrate base and sidewalls free from both condensate and frost dendrites. As the ice strips are elevated, frost atop them is in a

suspended state with a growth rate of an order of magnitude slower than that directly on the smooth surface. Recently, they adopt this concept to another regime by placing a clean surface in parallel with a prefrosted surface [73]. The clean surface can remain ice-free even in chilled and supersaturated conditions as a uniform out-of-plane dry zone covers it. Properly patterning icing stripes in the micrometer scale is necessary to fully explore its anti-frosting capacity. However, multiple delicate micromachining procedures as introduced are unlikely to apply in practical applications. Zuo et al. proposed a much simpler templating method to fabricate micrometer-sized parallel ice walls on any surface [72]. As shown in Figure 7c, three-dimensional ice walls engender local vapor sinks, attracting all nearby moisture on sidewalls and tops. The substrate base can remain uncontaminated from frost and condensate. A sustainable frost coverage of less than 13% is obtained. As ice walls can also be considered as fins, more heat transfer capacity is preserved when exposed to the same frost coverage.

3.5. Passive De-Frosting Methods via Reducing Ice Adhesion

Another frosting solution that reduces ice adhesion can also be applied if frost formation becomes inevitable. Surface engineering aiming to weaken the bonding strength between accumulated frost layers and substrate bases has been proven to be an effective passive de-frosting method. The ideal case is that the ice adhesion is so weak that frost layers can spontaneously be removed from the equipment surface under limited natural driven forces such as gravity.

Nanotextured superhydrophobic surfaces can resist the penetration of condensed microdrops, yielding a small solid–liquid contact. Accordingly, the resultant icing adhesion might be pronouncedly reduced than that of smooth surfaces. Ge et al. compared experimentally the bonding strength of an octadecyltrichlorosilane (OTS) superhydrophobic film and a smooth surface [74]. A mechanical sensor was employed to measure directly the bonding force of a frozen condensate drop on the prepared surface. The results show that OTS surfaces on average can reduce more than 95.74% of the bonding force, remaining icephobic even for a relatively large degree of supercooling. However, for microtextured superhydrophobic surfaces, condensed microdrops penetrate gaps and get locked after frozen, resulting in the formation of the impaled "Wenzel ice". An extremely large bonding strength 7 times higher than that of smooth surfaces was reported by Subramanyam et al. [75]. Therefore, tailoring surface textures to obtain the suspended "Cassie ice" is the key in the surface design to reduce ice adhesion.

Besides textured superhydrophobic surfaces, slippery liquid-infused porous surfaces (SLIPS) are very effective options in reducing ice adhesion. Kim et al. designed SLIPS by infusing a water-immiscible liquid into a nanotextured surface and obtained a bonding strength (~15.6 kPa) of 2 orders of magnitude lower than that of untreated aluminum surfaces(~1359 kPa) [76]. They attribute such low adhesion to the perfect smoothness of the ice-liquid interface which has very few defects or heterogeneities serving as pining spots. One possible failure of SLIPS is that the robustness can be compromised by losing the lubricant when exposed to strong shear flow or undergo repeating frosting/de-frosting cycles [77]. Liu et al. investigated extensively the effect of surface chemistry and topological features on their capability to retain the lubricant [78]. Their results show that a fluorinated hierarchical micro/nanoscale structured surface has the best performance in retaining the lubricant, while microscale and nanoscale pores fail to provide enough capillary forces to hold the lubricant.

4. Concluding Remarks and Future Perspectives

In this review, we have characterized the physical process of condensation frosting into five sequential stages, and provided an in-depth discussion of each stage. As frosting is undesired in most applications, we have also reviewed promising solutions to frosting problems, with a special focus placed on these newly developed anti-frosting methods.

Despite unprecedented advances in our understanding of the mechanism of condensation frosting and the development of many anti-frosting methods, we are still far from fully exploring its physics, and designing effective, eco-friendly, and low-cost anti-frosting surfaces is still a long-term goal. For example, many anti-frosting methods have been confirmed in laboratory conditions, but fail to meet harsh environments in applications. Condensation frosting, as one of the most important phase-change phenomena, needs to be further explored from both fundamental and application viewpoints.

Author Contributions: Conceptualization, T.G., Y.L. and Y.Z.; methodology, T.G., Y.L. and Y.Z.; formal analysis, T.G., Y.L. and Y.Z.; investigation, T.G. and Y.Z.; writing—original draft preparation, T.G. and Y.Z.; writing—review and editing, T.G. and Y.Z.; supervision, Y.Z.; funding acquisition, Y.Z. and D.W. All authors have read and agreed to the published version of the manuscript.

Data Availability Statement: Data sharing not applicable.

Conflicts of Interest: The authors declare no conflict of interest.

References

1. S., A.N. Snow Crystals. *Nature* **1888**, *37*, 343. [CrossRef]
2. Bigg, E.K. The formation of atmospheric ice crystals by the freezing of droplets. *Q. J. R. Meteorol. Soc.* **1953**, *79*, 510–519. [CrossRef]
3. Fletcher, N.H. Nucleation by Crystalline Particles. *J. Chem. Phys.* **1963**, *38*, 237–240. [CrossRef]
4. Laforte, J.L.; Allaire, M.A.; Laflamme, J. State-of-the-art on power line de-icing. *Atmos. Res.* **1998**, *46*, 143–158. [CrossRef]
5. De Koninck, L.H.; Ahmadi, S.F.; Boreyko, J.B. Passive anti-frosting cables. *Int. J. Heat Mass Transf.* **2020**, *146*, 118808. [CrossRef]
6. Cebeci, T.; Kafyeke, F. Aircraft Icing. *Annu. Rev. Fluid Mech.* **2003**, *35*, 11–21. [CrossRef]
7. Ding, L.; Chang, S.; Yi, X.; Song, M. Coupled thermo-mechanical analysis of stresses generated in impact ice during in-flight de-icing. *Appl. Therm. Eng.* **2020**, *181*, 115681. [CrossRef]
8. Li, K.; Xia, D.; Luo, S.; Zhao, Y.; Tu, R.; Zhou, X.; Zhang, H.; Su, L. An experimental investigation on the frosting and defrosting process of an outdoor heat exchanger in an air conditioning heat pump system for electric vehicles. *Appl. Therm. Eng.* **2022**, *201*, 117766. [CrossRef]
9. Hu, W.; Fan, J.; Song, M.; Jia, P.; Gao, Y. An experimental study on the frosting characteristic and performance of a micro-channel evaporator in an air source heat pump unit. *Energy Build.* **2020**, *224*, 110254. [CrossRef]
10. Lai, T.; Ding, P.; Dong, X.; Zhang, B.; Chen, X.; Hou, Y. Experimental study on the frosting characteristics of round tube in confined circular flow path at low temperature. *Appl. Therm. Eng.* **2020**, *171*, 115075. [CrossRef]
11. Pu, J.; Shen, C.; Zhang, C.; Liu, X. A semi-experimental method for evaluating frosting performance of air source heat pumps. *Renew. Energy* **2021**, *173*, 913–925. [CrossRef]
12. Seki, N.; Fukusako, S.; Matsuo, K.; Uemura, S. An analysis of incipient frost formation. *Warme Stoffubertrag.* **1985**, *19*, 9–18. [CrossRef]
13. Dooley, J.B. *Determination and Characterization of Ice Propagation Mechanisms on Surfaces Undergoing Dropwise Condensation*; Texas A&M University: College Station, TX, USA, 2010.
14. Guadarrama-Cetina, J.; Mongruel, A.; González-Viñas, W.; Beysens, D. Percolation-induced frost formation. *EPL (Europhys. Lett.)* **2013**, *101*, 16009. [CrossRef]
15. Lo, C.-W.; Li, J.-X.; Lu, M.-C. Frosting and defrosting on the hydrophilic nylon-6 nanofiber membrane–coated surfaces. *Appl. Therm. Eng.* **2021**, *184*, 116300. [CrossRef]
16. Liu, Z.; Ye, F.; Tao, H.; Lin, J. Effects of frost formation on the ice adhesion of micro-nano structure metal surface by femtosecond laser. *J. Colloid Interface Sci.* **2021**, *603*, 233–242. [CrossRef]
17. Jin, Y.; Soukane, S.; Ghaffour, N. Salt-solution-infused thin-film condenser for simultaneous anti-frost and solar-assisted atmospheric water harvesting. *Cell Rep. Phys. Sci.* **2021**, *2*, 100568. [CrossRef]
18. Lu, C.; Liu, C.; Yuan, Z.; Zhan, H.; Zhao, D.; Zhao, L.; Feng, S.; Liu, Y. Gradient droplet distribution promotes spontaneous formation of frost-free zone. *Commun. Mater.* **2022**, *3*, 80. [CrossRef]
19. Stefl, B.A.; George, K.F. Antifreezes and Deicing Fluids. In *Kirk-Othmer Encyclopedia of Chemical Technology*; John Wiley & Sons, Inc.: New York, NY, USA, 2000.
20. Walker, C.; Lerch, S.; Reininger, M.; Eghlidi, H.; Milionis, A.; Schutzius, T.M.; Poulikakos, D. Desublimation Frosting on Nanoengineered Surfaces. *ACS Nano* **2018**, *12*, 8288–8296. [CrossRef]

21. Boreyko, J.B.; Hansen, R.R.; Murphy, K.R.; Nath, S.; Retterer, S.T.; Collier, C.P. Controlling condensation and frost growth with chemical micropatterns. *Sci. Rep.* **2016**, *6*, 19131. [CrossRef]
22. Zhao, Y.; Yang, C. Retarded condensate freezing propagation on superhydrophobic surfaces patterned with micropillars. *Appl. Phys. Lett.* **2016**, *108*, 061605. [CrossRef]
23. Zhao, Y.; Wang, R.; Yang, C. Interdroplet freezing wave propagation of condensation frosting on micropillar patterned superhydrophobic surfaces of varying pitches. *Int. J. Heat Mass Transf.* **2017**, *108*, 1048–1056. [CrossRef]
24. Hou, Y.; Yu, M.; Shang, Y.; Zhou, P.; Song, R.; Xu, X.; Chen, X.; Wang, Z.; Yao, S. Suppressing Ice Nucleation of Supercooled Condensate with Biphilic Topography. *Phys. Rev. Lett.* **2018**, *120*, 075902. [CrossRef] [PubMed]
25. Boreyko, J.B.; Chen, C.-H. Self-Propelled Dropwise Condensate on Superhydrophobic Surfaces. *Phys. Rev. Lett.* **2009**, *103*, 184501. [CrossRef]
26. Boreyko, J.B.; Zhao, Y.; Chen, C.-H. Planar jumping-drop thermal diodes. *Appl. Phys. Lett.* **2011**, *99*, 234105. [CrossRef]
27. Miljkovic, N.; Preston, D.J.; Enright, R.; Wang, E.N. Electrostatic charging of jumping droplets. *Nat. Commun.* **2013**, *4*, 2517. [CrossRef] [PubMed]
28. Fletcher, N.H. Active Sites and Ice Crystal Nucleation. *J. Atmos. Sci.* **1969**, *26*, 1266–1271. [CrossRef]
29. Gurganus, C.; Kostinski, A.B.; Shaw, R.A. Fast imaging of freezing drops: No preference for nucleation at the contact line. *J. Phys. Chem. Lett.* **2011**, *2*, 1449–1454. [CrossRef]
30. Gurganus, C.; Kostinski, A.B.; Shaw, R.A. High-Speed Imaging of Freezing Drops: Still No Preference for the Contact Line. *J. Phys. Chem. C* **2013**, *117*, 6195–6200. [CrossRef]
31. Jung, S.; Tiwari, M.K.; Doan, N.V.; Poulikakos, D. Mechanism of supercooled droplet freezing on surfaces. *Nat. Commun.* **2012**, *3*, 615. [CrossRef]
32. Marín, A.G.; Enríquez, O.R.; Brunet, P.; Colinet, P.; Snoeijer, J.H. Universality of Tip Singularity Formation in Freezing Water Drops. *Phys. Rev. Lett.* **2014**, *113*, 054301. [CrossRef] [PubMed]
33. Jung, S.; Tiwari, M.K.; Poulikakos, D. Frost halos from supercooled water droplets. *Proc. Natl. Acad. Sci. USA* **2012**, *109*, 16073–16078. [CrossRef]
34. Zhao, Y.; Zuo, Z.; Tang, H.; Zhang, X. Ice Coverage Induced by Depositing a Water Drop onto the Supercooled Substrate at Extreme Low Vapor Pressure. *Crystals* **2021**, *11*, 691. [CrossRef]
35. Zhao, Y.; Zhu, F.; Zhang, H.; New, T.H.; Jin, L.; Yang, C. Triple condensate halo from a single water droplet impacting upon a cold surface. *Appl. Phys. Lett.* **2019**, *114*, 183703. [CrossRef]
36. Nath, S.; Ahmadi, S.F.; Boreyko, J.B. How ice bridges the gap. *Soft Matter* **2020**, *16*, 1156–1161. [CrossRef] [PubMed]
37. Boreyko, J.B.; Collier, C.P. Delayed Frost Growth on Jumping-Drop Superhydrophobic Surfaces. *ACS Nano* **2013**, *7*, 1618–1627. [CrossRef]
38. Hauer, L.; Wong, W.S.Y.; Sharifi-Aghili, A.; Kondic, L.; Vollmer, D. Frost spreading and pattern formation on microstructured surfaces. *Phys. Rev. E* **2021**, *104*, 044901. [CrossRef]
39. Zhao, Y.; Yang, C. Frost spreading on microscale wettability/morphology patterned surfaces. *Appl. Therm. Eng.* **2017**, *121*, 136–145. [CrossRef]
40. Zhao, Y.; Guo, Q.; Lin, T.; Cheng, P. A review of recent literature on icing phenomena: Transport mechanisms, their modulations and controls. *Int. J. Heat Mass Transf.* **2020**, *159*, 120074. [CrossRef]
41. Enriquez, O.R.; Marin, A.G.; Winkels, K.G.; Snoeijer, J.H. Freezing singularities in water drops. *Phys. Fluids* **2012**, *24*, 091102. [CrossRef]
42. Yu, F.; Liu, Z.; Li, Y.; Chen, Y.; Li, Y. Experimental study of frost crystal dendrite growth on a cryogenic cold surface under natural convection conditions. *Int. J. Refrig.* **2022**, *144*, 305–315. [CrossRef]
43. Huang, C.; Zhao, Y.; Gu, T. Ice dendrite growth atop a frozen drop under natural convection conditions. *Crystals* **2022**, *12*, 323. [CrossRef]
44. Zhang, L.; Song, M.; Deng, S.; Shen, J.; Dang, C. Frosting mechanism and behaviors on surfaces with simple geometries: A state-of-the-art literature review. *Appl. Therm. Eng.* **2022**, *215*, 118984. [CrossRef]
45. Sheng, W.; Liu, P.; Dang, C.; Liu, G. Review of restraint frost method on cold surface. *Renew. Sustain. Energy Rev.* **2017**, *79*, 806–813. [CrossRef]
46. Song, M.J.; Dang, C.B.; Liu, S.C.; Sun, Z.L.; Mao, N. Frost layer thickness measurement and calculation: A short review. *Energy Procedia* **2017**, *142*, 3812–3819. [CrossRef]
47. Byun, S.; Jeong, H.; Son, H.; Kim, D.R.; Lee, K.-S. Frost formation from general-low to ultra-low temperatures: A review. *Int. J. Heat Mass Transf.* **2022**, *195*, 123164. [CrossRef]
48. Yang, S.; Wu, C.; Zhao, G.; Sun, J.; Yao, X.; Ma, X.; Wang, Z. Condensation frosting and passive anti-frosting. *Cell Rep. Phys. Sci.* **2021**, *2*, 100474. [CrossRef]
49. Hermes, C.; Piucco, R.; Barbosa, J., Jr.; Melo, C. A study of frost growth and densification on flat surfaces. *Exp. Therm. Fluid Sci.* **2009**, *33*, 371–379. [CrossRef]
50. Song, M.; Shangwen, L.; Hosseini, S.H.; Luo, X.; Wang, Z. An experimental study on the effect of horizontal cold plate surface temperature on frosting characteristics under natural convection. *Appl. Therm. Eng.* **2022**, *211*, 118416. [CrossRef]
51. Wang, F.; Tang, R.; Wang, Z.; Yang, W. Experimental study on anti-frosting performance of superhydrophobic surface under high humidity conditions. *Appl. Therm. Eng.* **2022**, *217*, 119193. [CrossRef]

52. Shin, J.; Tikhonov, A.V.; Kim, C. Experimental Study on Frost Structure on Surfaces With Different Hydrophilicity: Density and Thermal Conductivity. *J. Heat Transf.* **2003**, *125*, 84–94. [CrossRef]

53. Tan, H.; Tao, T.; Xu, G.; Zhang, S.; Wang, D.; Luo, X. Experimental study on defrosting mechanism of intermittent ultrasonic resonance for a finned-tube evaporator. *Exp. Therm. Fluid Sci.* **2014**, *52*, 308–317. [CrossRef]

54. Dalili, N.; Edrisy, A.; Carriveau, R. A review of surface engineering issues critical to wind turbine performance. *Renew. Sustain. Energy Rev.* **2009**, *13*, 428–438. [CrossRef]

55. Hao, Q.; Pang, Y.; Zhao, Y.; Zhang, J.; Feng, J.; Yao, S. Mechanism of Delayed Frost Growth on Superhydrophobic Surfaces with Jumping Condensates: More Than Interdrop Freezing. *Langmuir* **2014**, *30*, 15416–15422. [CrossRef] [PubMed]

56. Wen, R.; Ying, Y.; Ma, X.; Yang, R. Sustainable anti-frosting surface for efficient thermal transport. *Cell Rep. Phys. Sci.* **2022**, *3*, 100937. [CrossRef]

57. Niroomand, S.; Fauchoux, M.T.; Simonson, C.J. The mechanisms of frost formation on a semipermeable membrane. *Int. J. Heat Mass Transf.* **2021**, *182*, 121912. [CrossRef]

58. Jung, S.; Dorrestijn, M.; Raps, D.; Das, A.; Megaridis, C.M.; Poulikakos, D. Are Superhydrophobic Surfaces Best for Icephobicity? *Langmuir* **2011**, *27*, 3059–3066. [CrossRef]

59. Ezzat, M.; Huang, C.-J. Zwitterionic polymer brush coatings with excellent anti-fog and anti-frost properties. *RSC Adv.* **2016**, *6*, 61695–61702. [CrossRef]

60. Grabowska, J.; Kuffel, A.; Zielkiewicz, J. Role of the Solvation Water in Remote Interactions of Hyperactive Antifreeze Proteins with the Surface of Ice. *J. Phys. Chem. B* **2019**, *123*, 8010–8018. [CrossRef]

61. Kasahara, K.; Waku, T.; Wilson, P.W.; Tonooka, T.; Hagiwara, Y. The Inhibition of Icing and Frosting on Glass Surfaces by the Coating of Polyethylene Glycol and Polypeptide Mimicking Antifreeze Protein. *Biomolecules* **2020**, *10*, 259. [CrossRef]

62. Yang, H.; Diao, Y.; Huang, B.; Li, K.; Wang, J. Metal–catechol complexes mediate ice nucleation. *Chem. Commun.* **2019**, *55*, 6413–6416. [CrossRef]

63. Huang, W.; Huang, J.; Guo, Z.; Liu, W. Icephobic/anti-icing properties of superhydrophobic surfaces. *Adv. Colloid Interface Sci.* **2022**, *304*, 102658. [CrossRef]

64. Nath, S.; Ahmadi, S.F.; Boreyko, J.B. A Review of Condensation Frosting. *Nanoscale Microscale Thermophys. Eng.* **2017**, *21*, 81–101. [CrossRef]

65. Zhao, G.; Zou, G.; Wang, W.; Geng, R.; Yan, X.; He, Z.; Liu, L.; Zhou, X.; Lv, J.; Wang, J. Competing Effects between Condensation and Self-Removal of Water Droplets Determine Antifrosting Performance of Superhydrophobic Surfaces. *ACS Appl. Mater. Interfaces* **2020**, *12*, 7805–7814. [CrossRef] [PubMed]

66. Mohammadian, B.; Annavarapu, R.K.; Raiyan, A.; Nemani, S.K.; Kim, S.; Wang, M.; Sojoudi, H. Delayed Frost Growth on Nanoporous Microstructured Surfaces Utilizing Jumping and Sweeping Condensates. *Langmuir* **2020**, *36*, 6635–6650. [CrossRef]

67. Zhao, Y.; Yan, Z.; Zhang, H.; Yang, C.; Cheng, P. Promote anti-/de- frosting by suppressing directional ice bridging. *Int. J. Heat Mass Transf.* **2021**, *165*, 120609. [CrossRef]

68. Chu, F.; Lin, Y.; Yan, X.; Wu, X. Quantitative relations between droplet jumping and anti-frosting effect on superhydrophobic surfaces. *Energy Build.* **2020**, *225*, 110315. [CrossRef]

69. Yao, Y.; Zhao, T.Y.; Machado, C.; Feldman, E.; Patankar, N.A.; Park, K.-C. Frost-free zone on macrotextured surfaces. *Proc. Natl. Acad. Sci. USA* **2020**, *117*, 6323. [CrossRef]

70. Jin, Y.; Wu, C.; Yang, Y.; Wu, J.; He, Z.; Wang, J. Inhibiting Condensation Freezing on Patterned Polyelectrolyte Coatings. *ACS Nano* **2020**, *14*, 5000–5007. [CrossRef] [PubMed]

71. Ahmadi, S.F.; Nath, S.; Iliff, G.J.; Srijanto, B.R.; Collier, C.P.; Yue, P.; Boreyko, J.B. Passive Antifrosting Surfaces Using Microscopic Ice Patterns. *ACS Appl. Mater. Interfaces* **2018**, *10*, 32874–32884. [CrossRef]

72. Zuo, Z.; Zhao, Y.; Li, K.; Zhang, H.; Yang, C. Suppressing condensation frosting using micropatterned ice walls. *Appl. Therm. Eng.* **2023**, *224*, 120099. [CrossRef]

73. Ahmadi, S.F.; Spohn, C.A.; Nath, S.; Boreyko, J.B. Suppressing Condensation Frosting Using an Out-of-Plane Dry Zone. *Langmuir* **2020**, *36*, 15603–15609. [CrossRef] [PubMed]

74. Ge, L.; Ding, G.; Wang, H.; Yao, J.; Cheng, P.; Wang, Y. Anti-Icing Property of Superhydrophobic Octadecyltrichlorosilane Film and Its Ice Adhesion Strength. *J. Nanomater.* **2013**, *2013*, 5. [CrossRef]

75. Bengaluru Subramanyam, S.; Kondrashov, V.; Rühe, J.; Varanasi, K.K. Low Ice Adhesion on Nano-Textured Superhydrophobic Surfaces under Supersaturated Conditions. *ACS Appl. Mater. Interfaces* **2016**, *8*, 12583–12587. [CrossRef]

76. Kim, P.; Wong, T.-S.; Alvarenga, J.; Kreder, M.J.; Adorno-Martinez, W.E.; Aizenberg, J. Liquid-Infused Nanostructured Surfaces with Extreme Anti-Ice and Anti-Frost Performance. *ACS Nano* **2012**, *6*, 6569–6577. [CrossRef]

77. Kim, P.; Kreder, M.J.; Alvarenga, J.; Aizenberg, J. Hierarchical or Not? Effect of the Length Scale and Hierarchy of the Surface Roughness on Omniphobicity of Lubricant-Infused Substrates. *Nano Lett.* **2013**, *13*, 1793–1799. [CrossRef] [PubMed]

78. Liu, Q.; Yang, Y.; Huang, M.; Zhou, Y.; Liu, Y.; Liang, X. Durability of a lubricant-infused Electrospray Silicon Rubber surface as an anti-icing coating. *Appl. Surf. Sci.* **2015**, *346*, 68–76. [CrossRef]